*Journal of Nano Research*
*ISSN: 1661-9897, Vol. 80, pp 1-19*

*Submitted: 2023-01-31*
*Revised: 2023-06-18*
*Accepted: 2023-06-29*
*Online: 2023-09-05*

# Photocatalytic Degradation of Orange II by Active Layers of Ag-Doped CuO Deposited by Spin-Coating Method

Zerouali Madiha[1,a], Daira Radouane[1,b*], Dikra Bouras[2,c], Boudjema Bouzid[1,d] and Régis Barillé[3,e]

[1]LRPCSI, University 20 Août 1955, Skikda, P.B. 26, route d'El-Hadaiek, 21000, Skikda, Algeria

[2]Laboratory of Active Components and Materials, University of Oum El Bouagh, Oum El Bouaghi 04000, Algeria

[3]MOLTECH-Anjou, University of Angers/UMR CNRS 6200, 2 Bd Lavoisier, 49045 Angers, France

[a]zeroualimadiha20@gmail.com, [b]daira_radouane@yahoo.fr, [c]bouras.dhikra@yahoo.fr; [d]boudjema_b@yahoo.fr, [e]regis.barille@univ-angers.fr

**Keywords:** Ag:CuO, Spin-coating, Photocatalysis, Energy gap, Impurity removal.

**Abstract:** For water purification in our daily life at low cost and in the goal to study the effect of doping elements for heterogeneous photocatalysis application, thin layers of Ag doped CuO, (5, 15, 25 and 50 wt.%) were prepared by a sol-gel method on a glass substrate for photocatalysis. The structural, morphological, optical and electrical characteristics of these layers have been studied. The results of X-ray diffraction (XRD) proved that there was a monoclinic phase structure in the direction (-111). This result indicated that thin films are polycrystalline. It was confirmed by infrared spectra (IR). In the case of Ag doping, scanning electron microscope (SEM) revealed a change in the shape of the granules with large and inhomogeneous sizes. Granules were spherical in the case of pure copper oxide. The energy gap decreases from 2.17 eV to 1.25 eV with the increasing doping. The improved capacitance is explained in terms of Ag particles present in CuO nanostructures giving a good electrical conductivity. The doping effect of Ag ions has improved the photocatalytic property of the CuO. It was tested for organic dye cleaning with Orange II. In addition, the presence of pores on the surface of Ag:CuO thin films and a reduce energy gap enables the creation of a greater number of •O and •OH that leads to eliminate the dye and give a transparent solution. A 50 wt.% Ag doping showed a high photoactivity (43%)after 5h compared to a pure CuO thin film (27% of degradation rate) for the same time.

## 1. Introduction

The textile industry is known to be polluting because its discharges consist of recalcitrant organic molecules that cannot be treated by conventional methods of decontamination. Synthetic dyes, 15% of which consist of nitrogen dyes, are among the most important sources of water pollution[1]. Despite great efforts in wastewater treatment, it is still unfortunately estimated that only 60% of the polluted water is sent to the treatment plant, and the rest is discharged into natural environment. One of the most alarming phenomena is the increasing accumulation of recalcitrant substances that are difficult to eliminate in water [2]. The situation is exacerbated by the lack or inadequacy of appropriate water treatment systems able to reduce the concentration of toxic substances that are chronic chemical hazards [3]. Organic pollutants present in wastewater, such as dyes, petroleum, and pharmaceuticals, are an environmental problem in modern society [4]. Organic pollutants in water have the potential to have a negative impact on health and increase the risk of chronic diseases. Moreover, in many countries pollution from textile industry discharges is heavily spread with dyes [5]. Dyes are often used in excess to improve colors; As a result, wastewater is highly concentrated in pigments, making it difficult to environmentally apply degrading biological treatments [6].

It is therefore necessary to find an effective method to remove these pollutants from wastewater from the textile, tanning or printing industries. A number of procedures and techniques including membrane filtration, adsorption, coagulation or flocculation, electrochemical oxidation processes

and biodegradation have been documented [7]. More than 15% of the dyes produced worldwide for the textile industry are azo dyes such as Orange II (OII). Azo dyes are the largest and most versatile class of organic dye-stuffs. These contain one or more azo bonds (–N=N–) as a chromophore group in association with aromatic structures containing functional groups such as –OH and $–SO_3H$ [4]. The complex aromatic structures of azo dyes make them more stable and more difficult to remove from the effluents discharged into the water bodies [8]. Thus, the removal of these dyes from wastewater is an important target from the environmental point of view. Currently, some typical non-destructive treatments, such as integrated processes that combine different combinations of biological, physical and chemical whitening, are used to reduce the amount of these pigments, which are essentially non-biodegradable and toxic. OII is an azo dye for textiles that resists fading by light, common acids and bases [9].Alternative names for OII are Acid Orange 7 and Acid Orange II [10]. Heterogeneous photo catalysis, which allows the elimination of organic pollutants such as dyes while leading to complete mineralization, seems to be an alternative technology. The main factors influencing the photocatalytic process are the characteristics of the molecule to be broken down, the light source and the type of semiconductor acting as the photocatalyst (gap and texture) [11].

The sol-gel method makes it possible to produce a wide variety of oxides in different configurations: monoliths [12], thin films [13] and powders [14]. This process is very attractive, because it gives the possibility of diversified shaping of materials. It is used in several technological fields, optics, electronics and biomaterials. This method has the advantage of using soft chemistry; it makes it possible to obtain very pure and stoichiometric materials. The solution - gelation consists of a solution based on precursors in the liquid phase which is transformed into a solid by a sum of chemical reactions of the polymerization type at room temperature. Thin layers can be manufactured and prepared by several deposition techniques such as spray pyrolysis [15], dip-coating [16] and spin-coating [17], DC reactive sputtering [18] and thermal evaporation [19]. The last one is an inexpensive technique that allows a variety of materials to be obtained. The main advantages of this method are the good homogeneity, the ease of controlling the chemical compositions, the used heat treatment at low temperature (400-600 °C) and the good optical method [15].

In previous studies, Ag-CuO thin films were successfully used for photodegradation of dyes due to the recycling ability of microgels [6, 20]. Also a significant visible-light-driven photocatalyst for environmental remediation was obtained [21]. For this reason, the present study has been focused on the se effective elements (Ag, CuO).

The use of Copper oxide (CuO) in the photocatalytic destruction of environmental organic contaminants has attracted considerable interest. So far, the CuO photocatalyst has been efficiently produced in a variety of morphologies, including nanorods, nanoplates, nanotubes, hollow microspheres, microsprays, and nanowires [22]. CuO is an excellent candidate for semiconductor catalysts [21]and has advantages of being non-toxic, economical and environmentally friendly. The simple oxide formation makes the material attractive [23]. Due to the availability of its components in nature, its inexpensive manufacturing, superior thermal stability and electrochemical characteristics, it is an excellent candidate for semiconductor photocatalysts [22].In addition, it has good optical and electrical properties and a high conductivity [24]. CuO is crystallized in a tenorite-like monoclinic structure with lattice parameters a= 4.6Å,b=3.4Å,c=5.1Å and β=99.2Å [25],a direct band gap (Eg = 1.2 to 2.2 eV) [26],a refractive index = 1.4 and an ionic radius 0.73Å [27].The copper oxide films were prepared used in a number of applications such as gas sensor [28], antibacterial activity [29], solar cell [30] and photocatalysis [31]. Copper (Cu) has different oxidation states, such as $Cu^{1+}$, $Cu^{2+}$ and $Cu^{3+}$, which makes it equally promising for hole and electron doping. Nowadays, CuO is used as a photocatalyst, antioxidant, and drug delivery agent and imaging mediator in the field of biomedicine [32-34].

Ag atom doping has been widely attracted by researchers due to its novel applications in high density optical storage devices [35], gas sensors [36], photovoltaic cells [37], photodiodes and antibacterial coatings [38, 39]. Recently, silver oxide ($Ag_2O$) with a low energy bandgap (1.3 eV)

has received more attention in the practical photocatalytic application, due to ist great capacity in absorbing NIR light with out further process [40]. Moreover, on the basis of its relative high VB edge (1.5 eV vs NHE), it is feasible to drive necessary oxidation reaction for the split of water or degradation of organic pollutant molecules [41]. In order to determine the doping efficiency and their impact on photocatalysis, the application of photocatalysis by the degradation of OII under UV irradiation with catalysts in thin layers of CuO doped with Ag prepared by a sol-gel spin coating method is studied. The obtained results show that the use of thin layers of CuO doped with Ag causes the degradation of a dye (OII) at a rate of up to 43% for 5 h .This result indicates that Ag enhanced the photocatalyzed degradation due its optical property and its small energy gap compared to pure CuO.

## 2. Experimental Study

### 2.1. Materials

Dehydrated copper acetate($Cu(CH_3COO)_2.2H_2O$), absolute ethanol ($C_2H_6O$; purity96%)and monoethanolamine (MEA;$NH_2CH_2CH_2OH$≥98%) are used for the prepared solution. Silver nitrate ($AgNO_3$; purity 99%)is used for doping.OII ($C_{16}H_{11}N_2NaO_4S$; OII)as organic dye for photocatalysis application is provided by Sigma-aldricht.

### 2.2. Preparation of thin layers

The thin layers were deposited by the sol-gel spin coating method and consists in a thin film of a solution deposited on a glass substrate (2cm× 2 cm)by centrifugation. In order, to prepare the 0.2M solution the dehydrated copper acetate precursor is dissolving in absolute ethanol. For studying the effect of doping rate by Ag on the thin layers of CuO, four different silver percentage solutions of (n(Ag)\ n(Cu))*100% =X%)with X= 5, 15, 25 and 50 with silver nitrate precursor $AgNO_3$ were prepared. A volume of monoethanolamine (MEA) was added in a molar ratio (n (MEA) \ n (sol) = 3). The solution was then heated under magnetic stirring at 70°C for 2 h.
All substrates were cleaned with methanol and distilled water for 5min and then dried, put in the oven at a temperature of 50°C for 10min. The spin-coating precursor solutions (2ml using a syringe) were dropped on substrates with a rotating speed of 3000 rpm for 30 s, followed by drying after each deposition at 250°C for 10 min in the oven. This cycle was repeated 4 times. Then a calcination in the oven was done at 500°C for 2 h.

### 2.3. Characterization techniques

In the goal to study the structural properties of thin layers of pure and Ag-doped CuO, XRD (Schimadzu Brucker AXS D8 ADVANCE type with a Cu Kα radiation diffractometer (λ = 1.54Å)) was used. The absorption spectra of the photocatalysts were obtained with a UV – visible spectrophotometer (model V-750) in the wavelength range 250-900 nm. The morphology of the films was examined using an environmental scanning electron microscope SEM type Thermo scientific Prisma E. The IR transmission spectra were recorded using a VERTEX 70 spectrophotometer in the spectral range [400 – 3600] $cm^{-1}$. The electrical properties were done with a four-point measuring device, JANDEL model, connected to a Keithley 2400 source meter.

## 3. Results and Discussion

### 3.1. X Ray Diffraction

Figure (1) represents the XRD spectra of thin films of Ag-doped CuO (Ag:CuO) recorded in the 2θ range from 25° to 70°. it presents several diffraction peaks attributed to the following crystal planes (110), (-111),(200),(-202), (020), (202),(-113),(-311),(220).The results are in agreement with the

JCPDS file code 00-041-0254 and confirm the presence of a tenorite phase of monoclinic structure, which belongs to space group $C_2/c$. After Ag doping exceeding 5%, there are additional peaks corresponding to the presence of the related secondary phases in the doped CuO films. The existence of the $Ag_2O$ phase given by the four diffraction peaks found at the values 2θ =27.77°,38.26°,54.68°, and 64.55° correspond to the planes (110), (200), (211), (311) respectively and agree well with the JCPDS file (code00-041-1104).The peak (440) is in agreement with the JCPDS card (code00-040-0909) indicating the formation of silver oxide $Ag_2O_3$.
Because of an addition of Ag atoms, there is a definite shift in the position of these peaks towards lower angles.This shift indicates that Ag atoms of ionic radius 1.15 Å occupied the substitutional site of the $Cu^{2+}$ atoms of ionic radius 0.73Å [42, 43] and involve a dilation in the CuO crystal lattice.

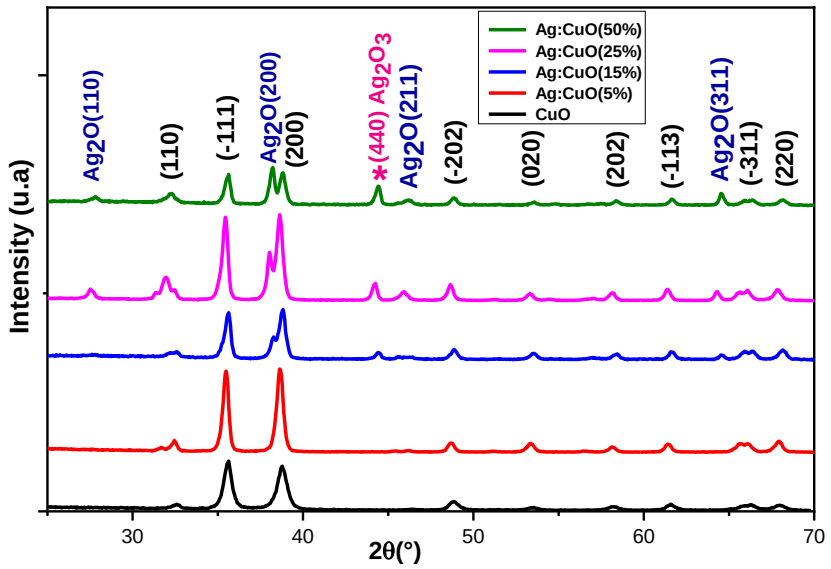


Fig.1.XRD spectra of thin layers of Copper oxide doped with different percentages of silver.

The crystallite sizes are nanometric varying from 16 nm to 24 nm and increase with the increase of doping thanks to the ionic radius of the silver atom (Fig.2). Similar results have been found in several studies of increasing crystal size of CuO doped with silver [44, 45]. Ag doping CuO improved the crystallinity of these layers with an increase in the crystal size and a decrease in strain. The crystallite sizes of these layers are illustrated in Table 1 and were calculated with the Scherrer's equation [46]:

$$D = \frac{0.9 \cdot \lambda}{\beta \cdot cos\theta} \quad (1)$$

where D is the size of the crystallites, λthe wavelength of the incident ray,β the width at half maximum (FWHM) and θthe Bragg diffraction angle.
The micro-strain (ε) created in the thin films was calculated by relation ship[47]:

$$\varepsilon = \frac{\beta \cdot cos\theta}{4} \quad (2)$$

Table 1. The crystallite size of the samples

| Phases | Plan (hkl) | 2θ (°) | θ(°) | FHWM β(°) | β (rad) | D (nm) | $\varepsilon.10^{-2}$ |
|---|---|---|---|---|---|---|---|
| **CuO** | (-111) | 35.561 | 17.781 | 0.493 | 0.0086 | 16 | 0.215 |
| **Ag :CuO (5%)** | (-111) | 35.526 | 17.763 | 0.378 | 0.0066 | 21 | 0.165 |
| **Ag :CuO (15%)** | (-111) | 35.583 | 17.792 | 0.361 | 0.0063 | 22 | 0. 157 |
| **Ag :CuO (25%)** | (-111) | 35.486 | 17.743 | 0 .344 | 0.0060 | 23 | 0.150 |
| **Ag :CuO (50%)** | (-111) | 35.573 | 17.787 | 0.326 | 0.0057 | 24 | 0.142 |

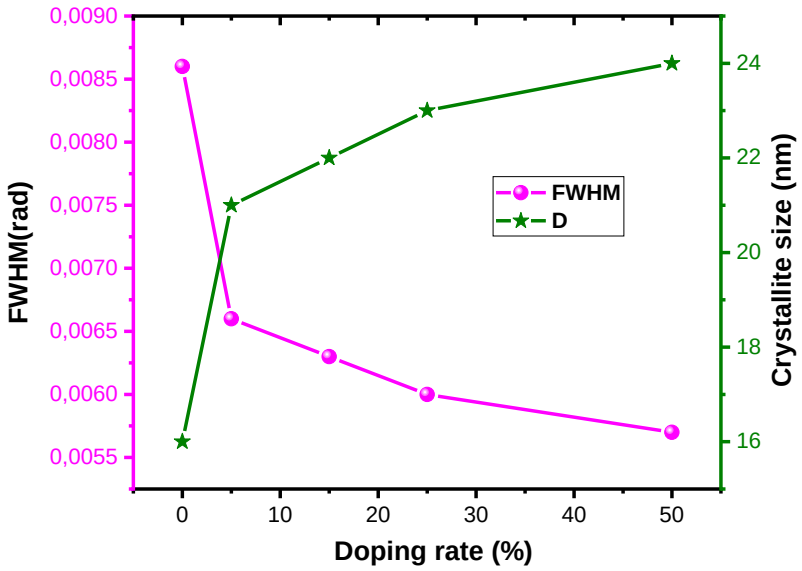


Fig. 2.Variation of crystallite size and FWHM of Ag:CuO samples as a function of the doping rate.

In order to know the change of axes (x, y), the lattice parameters ($a \neq b \neq c$, $\alpha = \gamma = 90° \neq \beta$) of the monoclinic structure of CuO were calculated using the following equations[48, 49]:

$$\frac{1}{d^2} = \frac{1}{sin^2\beta}\left(\frac{h^2}{a^2} + \frac{k^2 sin^2\beta}{b^2} + \frac{l^2}{c^2} - \frac{2hlcos\beta}{ac}\right) \quad (3)$$

From the lattice parameter values indicated in table 2, it is noted an increase of lattice parameters (a, b), angles β and volumes of the crystallattice in all the thin films doped with silver. This result indicates the presence of a dilation of the lattice.

Table 2. The lattice parameters a, b and c

| Phases | a( Å) | b( Å) | c( Å) | β (°) | v ( $Å^3$) |
|---|---|---|---|---|---|
| **CuO** | 4.698 | 3.417 | 5.119 | 99.41 | 80.71 |
| **Ag :CuO (5%)** | 4.728 | 3.426 | 5.079 | 99.47 | 81.14 |
| **Ag :CuO (15%)** | 4.709 | 3.426 | 5.075 | 99.44 | 80.94 |
| **Ag :CuO (25%)** | 4.709 | 3.426 | 5.102 | 99.60 | 81.23 |
| **Ag :CuO (50%)** | 4.691 | 3.416 | 5.098 | 99.50 | 80.81 |

### 3.2. SEM Analysis

The study of the surface morphology by the SEM was carried out on the thin films of Ag-doped CuO. all the films showed a dense deposition and the surfaces are covered with almost a homogeneous and uniform grain size which clearly show the formation of a crack-free surface.

Figure 3 shows nano-spherical grains in the case of pure copper oxide. When the doping is present; there is a clear change in the shape of the grains after the addition of Ag. It is observed from SEM images that this change is strongly dependent on the percentage of doping. Moreover, the presence of large pores and in greater number with an increase in the doping rate confirms that Ag gives a more porous surface. It was also observed that there was an increase in the number and in the average size of pores. The value of the pore sizes changed from 43 nm (for pure CuO) to 193 nm (with 50 wt.% Ag:CuO). The addition of silver into CuO has contributed significantly to the increase in the percentage of pores within the granules and induced the capture of a larger number of impurities in the dye.

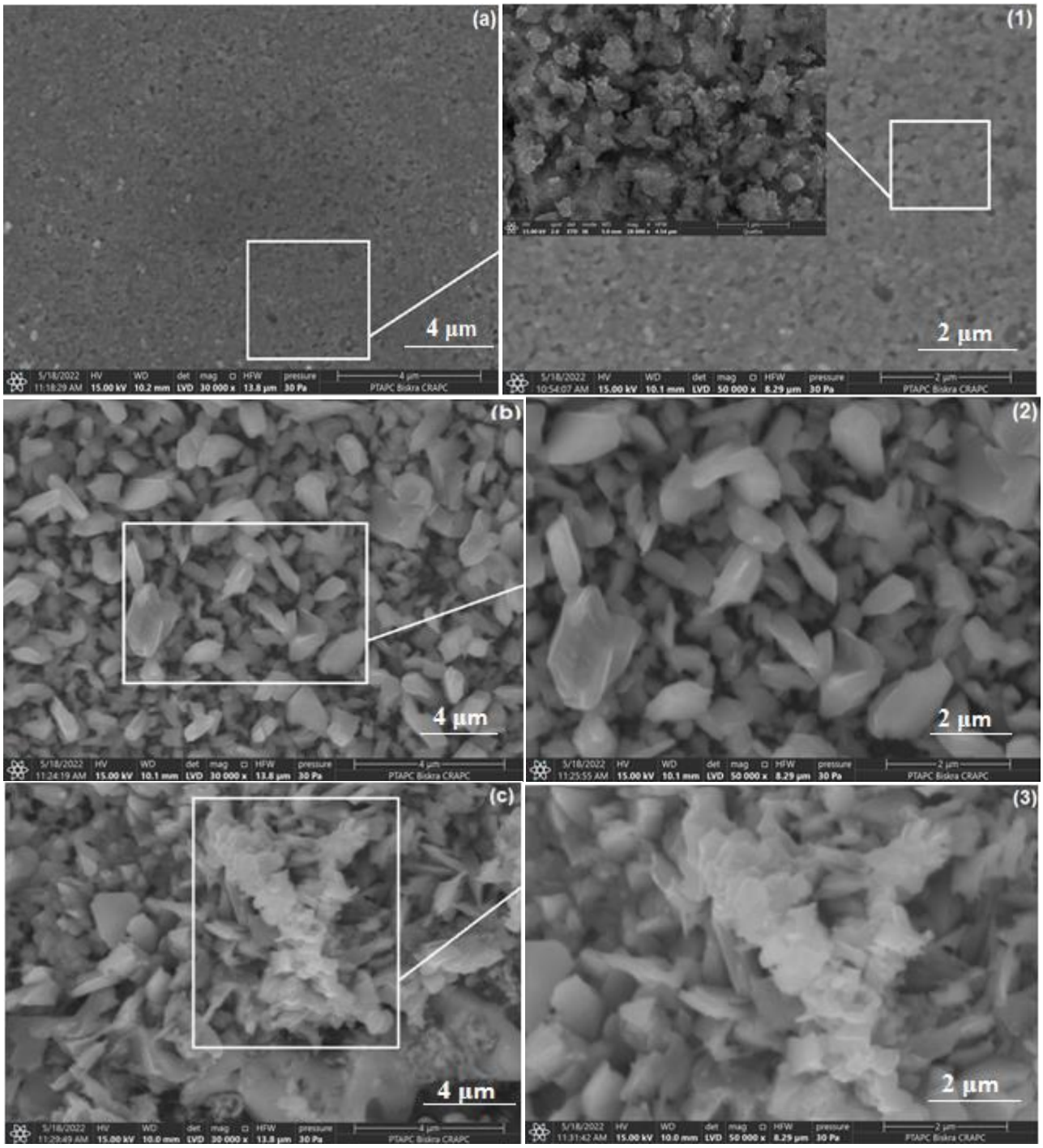

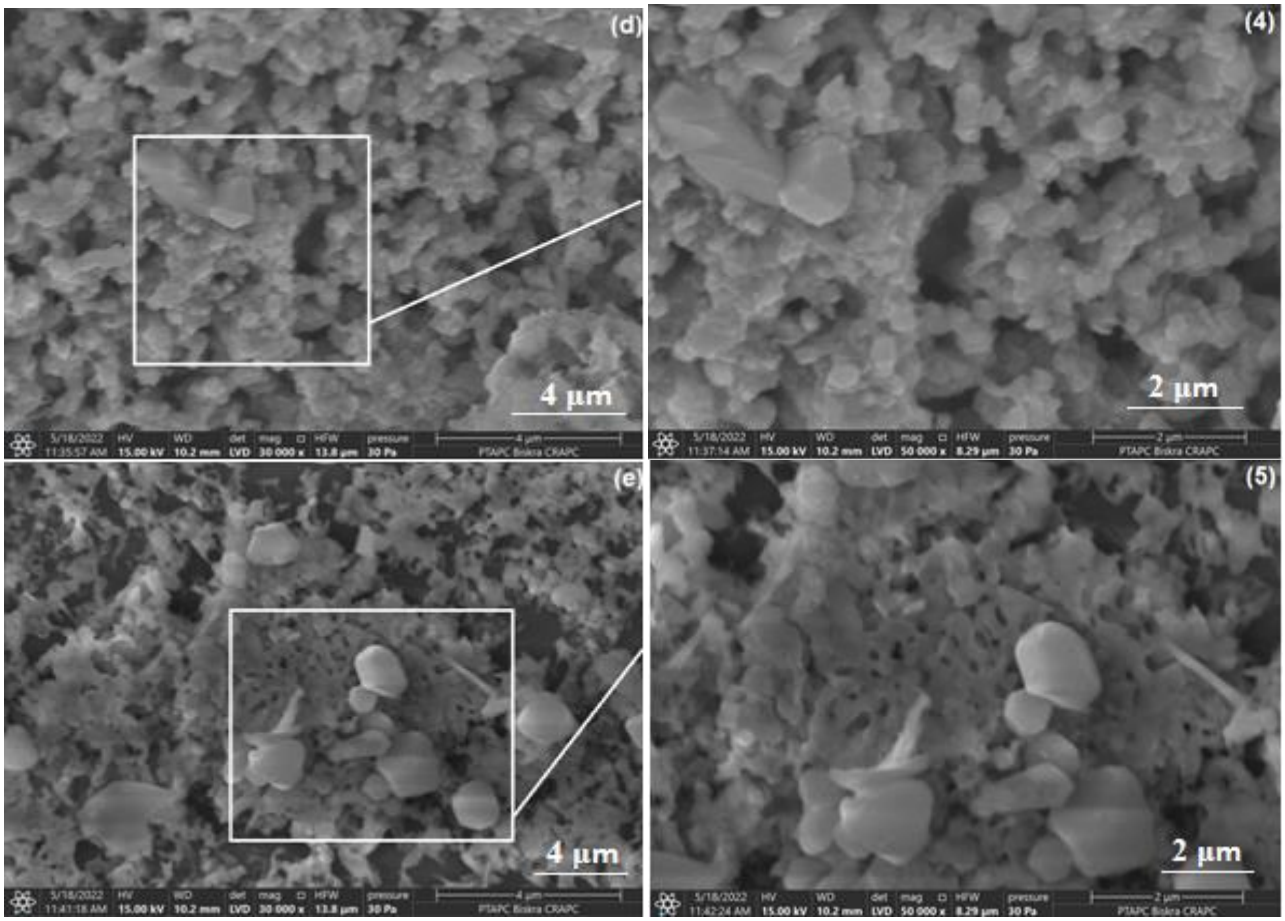


Fig.3. SEM image of various prepared samples. CuO (a),5 % Ag:CuO (b),15 % Ag :CuO (c) 25 % Ag:CuO (d), 50 % Ag:CuO (e),zoom of4µm x 4µm CuO (1),5 % Ag:CuO (2),15 % Ag:CuO (3), 25 % Ag:CuO (4),zoom of 2µm x 2µm 50 % Ag:CuO (5).

### 3.3. EDX Analysis

In order to confirm the presence of silver doping and the chemical composition of the thin layers, a EDX analysis was used. The spectra of Ag:CuO thin films with different doping ratios are shown in Table3. The Cu and O are clearly visible throughout the samples. The presence of additional Ag element also increases with the increase in the doping rate (1.28%fordoping with 15% Ag, 33.83 % for doping with 25% Ag and 38.03%fordoping with 50% Ag).Except for the rate of 5%Ag, silver was not sensed and this could be due to the low added rate of doping.

This result is in good agreement with the XRD results and confirms the production of CuO and $Ag_2O$ on the brightening of the glass substrate.

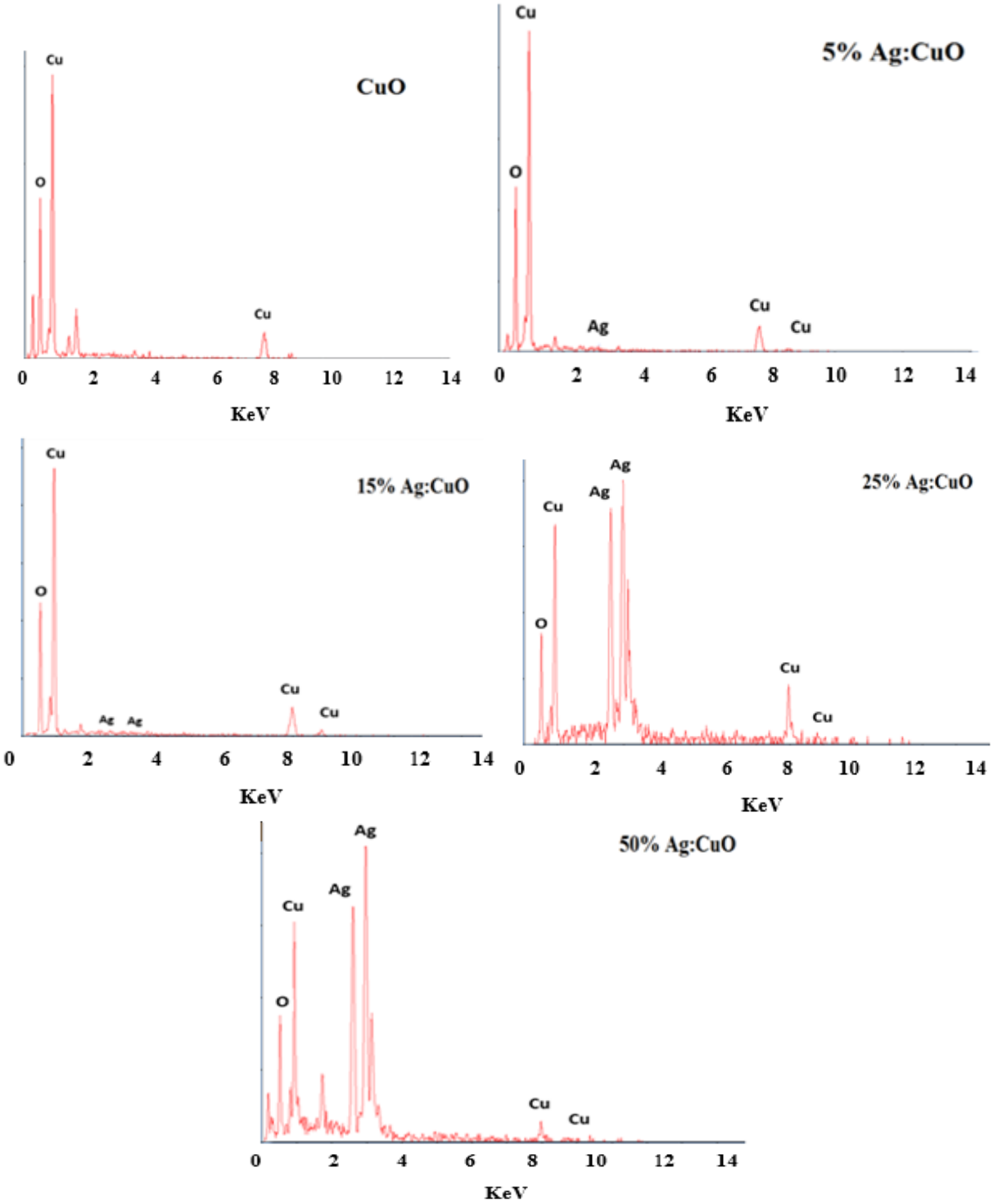


Fig 4. EDX analysis spectrum of for thin films of CuO undoped and doped with silver.

**Table 3.** Percentage of atoms present in EDX spectrum.

| Phases | Cu% | O% | Ag% |
|---|---|---|---|
| **CuO** | 44.04 | 55.96 | 0 |
| **Ag :CuO (5%)** | 58.36 | 41.62 | 0.02 |
| **Ag :CuO (15%)** | 43.6 | 55.12 | 1.28 |
| **Ag :CuO (25%)** | 18.61 | 47.56 | 33.83 |
| **Ag :CuO (50%)** | 6.06 | 55.91 | 38.03 |

### 3.4. Vibrational Spectroscopy

The IR technique has been used to characterize thin films in order to gain a better understanding of the chemical compositions of the samples and the interactions that determine the attributes of the samples. Infrared (IR) spectra of undoped and Ag-doped CuO thin layers were recorded in the range 400-3000 $cm^{-1}$. Figure 5 shows, several absorption bands clearly identified. The absorption peaks detected at 472, 616, 667 and 718 $cm^{-1}$ correspond to Cu-O bonding in the characteristic stretching vibrations of CuO [50].
After doping with silver (15%, 25% and 50%), we notice a big difference in the absorption spectra in the 400-1100$cm^{-1}$range. The peaks of708 $cm^{-1}$,804 $cm^{-1}$,866 $cm^{-1}$ and 1147 $cm^{-1}$ are characterized by Ag-O binding and the other peak of 460$cm^{-1}$ characterized by Ag binding Ag-O-Ag [39].A strong bond is observed peak at 1742$cm^{-1}$and represents the mode of C=O bond stretching vibrations. The peaks at 1641 $cm^{-1}$ corresponding to the vibration of the H-O-H bond which are associated with the vibration mode hydroxyl groups bound to adsorbed water [51].The bands observed around 1110 $cm^{-1}$ and 1155$cm^{-1}$can be attributed to the presence of asymmetric Si-O-Si stretching vibrations [52].

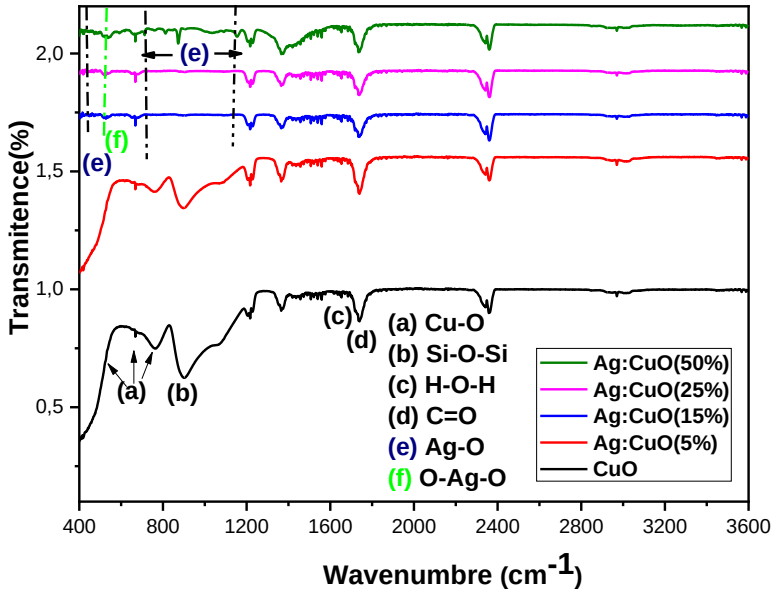


Fig.5.Infrared spectra of the Ag doped CuO with different percentage

### 3.5. Optical properties

#### 3.5.1. Absorbance spectra

Thin layers of undoped and Ag-doped CuO were optically analyzed by UV Vis spectrophotometer. Figure 6 depicts the absorption spectra performed in the 250 – 900nm wavelength range. All spectra show absorbing in the visible and near IR [53]. It should be observed that the thin layers of pure CuO exhibit the lowest absorbance compared to the samples after doping. The addition of Ag with different percentages in CuO thin films significantly increased the absorption.
The absorption spectra showed strong absorption peaks around 310 nm and 360 nm with an absorption edge around 750 nm which corresponds to the CuO band transition. this shows that CuO films are crystalline [54]. It is observed that the absorption peaks of the thin layers of Ag:CuO is shifted to a higher wavelength corresponding to a decrease in the value of the band gap [55]. The absorption is maximum for thin films of Ag doped in the visible range. For pure copper oxide the absorption is maximum in the near IR range. This result shows that the doping by the Ag element widens the absorption zone from the near IR domain to the visible domain.

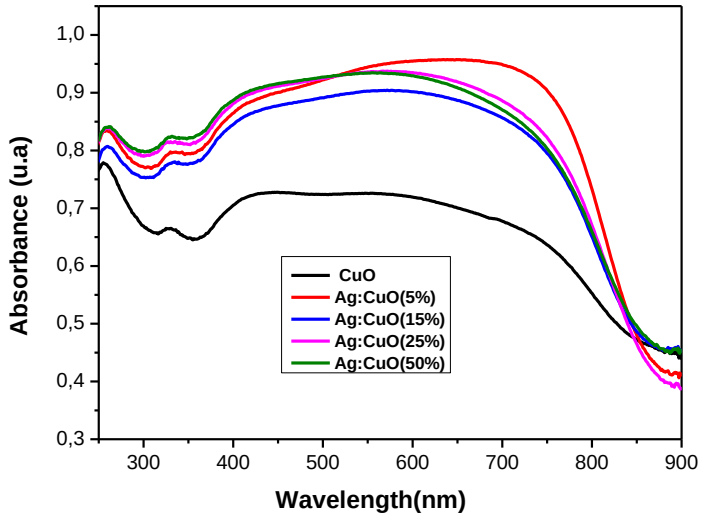


Fig.6. Absorbance spectra of CuO thin layers doped with Ag (0%, 5%, 15%, 25% and 50%).

### 3.5.2. Energy Gap

In order to determine the energy gap of the thin layers prepared by the spin-coating method, the following Tauc equation is used [56]:

$$\alpha h\nu = A \cdot \left(h\nu - E_g\right)^{1/2} \quad (4)$$

with A: Constant, Eg: Optical Gap in eV, hν: energy of a photon eV.
Figure 7 shows the plot of $(\alpha h\nu)^2$ as a function of the energy of a photon $h\nu$.With the extrapolation method, the optical gaps $E_g$ are extracted.

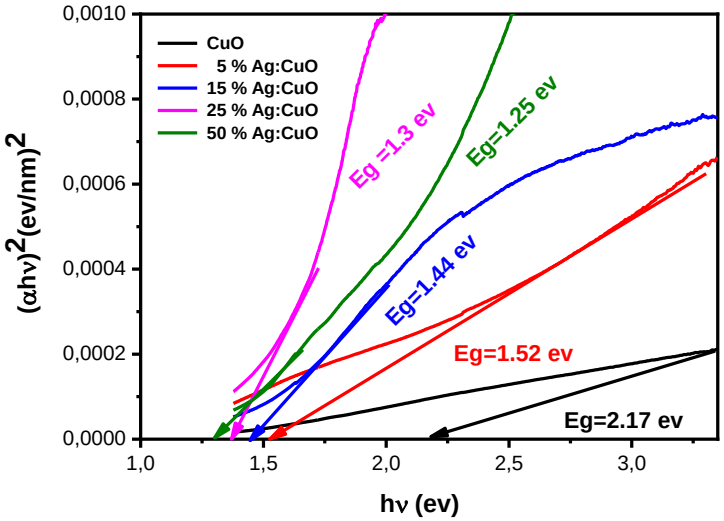


Fig.7.Variation of $(\alpha h\nu)^2$ as a function of photon energy of Ag doped CuO thin layers.

The energy gap values range from 2.17 eV up to 1.25 eV with an increasing Ag doping rate (Fig.7). This decrease is explained by the fact that doping leads to the displacement of the absorption edge towards lower energies. This is due to an increase in generating energy levels above the valence band. This result confirms that the displacement of Fermi levels towards the valence band (VB) gives to the Ag-doped CuO a P-type semiconductor. This result leads to the absorption of photons of lower energy, and therefore to an increase in transitions electronics and then a decrease in the values of the energy gap.

### 3.6. Electrical properties

The four-point method is used to measure the electrical conductivity (σ) and electrical resistivity (ρ) of Ag:CuO thin films. The conductivity value is computed using the formula below [48]:

$$\rho = \frac{\Delta v}{I}.e.\frac{\pi}{Ln2} \quad (5)$$

The electrical conductivity increases with an increase in the case of doped with silver, as the conductivity of the undoped CuO is$3.5.10^{-5}\Omega^{-1}\cdot cm^{-1}$, while in the presence of silver it increase until they reach a value of $5.2.10^{-4}\Omega^{-1}\cdot cm^{-1}$for the 50 % Ag:CuO. The resistance values are decreasing in the presence of doping. The results are shown in Table 4.

Table 4. The electrical parameters obtained by the 4-point method.

| | **e(nm)** | $\boldsymbol{\rho(\Omega \cdot cm)}$ | $\boldsymbol{\sigma(\Omega^{-1}\cdot cm^{-1})}$ |
|---|---|---|---|
| **CuO pure** | 320 | 28016.42 | $3.5.10^{-5}$ |
| **5 %Ag :CuO** | 338 | 16193.5 | $6.175 .10^{-5}$ |
| **15 %Ag :CuO** | 412 | 12561.88 | $7.9.10^{-5}$ |
| **25 %Ag :CuO** | 443 | 4728.45 | $2.1.10^{-4}$ |
| **50 %Ag : CuO** | 670 | 1922.85 | $5.2.10^{-4}$ |

Figure 8 shows the variation of conductivity and electrical resistivity of CuO:Ag films as a function of Ag concentration. The results can be due to the evolution of the resistivity for the greatest defect density at the grain boundaries due to the differences in the presence of the atoms of Cu and Ag, and the difference of surface shape. The values of electrical conductivity well agreed with results given in references [56]. It also shows that the conductivity of the samples increases with increasing concentration of silver doping. This observation leads to an increase in the charge carriers responsible for electrical transport. An increase in the electrical conductivity is associated also with an increase in the crystal size and thus a decrease in the grain boundaries, which leads to a decrease in the energy levels and thus the ease of movement of charge carriers. There is an inverse relationship between the crystallite size and energy gap. It can be explained by a quantum confinement size effect [49]. In addition to this effect, the thickness of CuO thin films which acted as the active layer was considered as an important factor for studying the effect on the electrical properties [48].

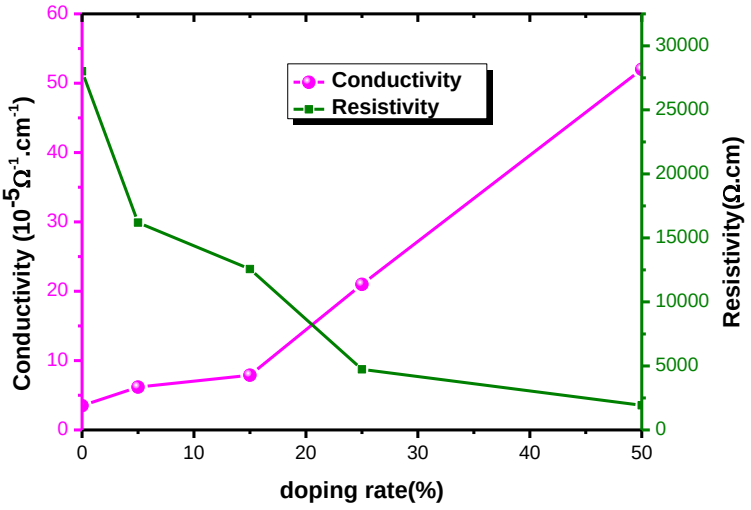


Fig.8. Variation of conductivity and resistivity as a function of doping ratio by 4 points technique

### 3.7. Photocatalytic Performance

The optical, structural and morphological characteristics of thin films CuO, 5% Ag:CuO, 15% Ag:CuO, 25% Ag:CuO and 50% Ag:CuO have a significant influence on the photocatalytic performances. The samples are influenced by their band gap, light absorption capacity, crystallinity and surface [57].

Heterogeneous photocatalysis is based on the absorption of photons with energy greater than or equal to the width of the forbidden band ($h\nu \geq Eg$) of the semiconductor were studied [58]. Such as the electrons which are in the band of valence passed to the band of conduction and smoothed a hole in the band of valence for creation of the pair (e-/h+). In the goal to generate hydroxyl radicals (OH•), holes in the valence band interact with anions ($OH^-$). Super oxide radicals $\bullet O_2^-$ are formed when electrons in the conduction band interact with oxygen molecules $O_2$, and gives the transparent solution (Equation 6) which increased when active layers were deposited with low gaps.

$$\bullet O_2^- + OH\bullet + \text{Dye} \rightarrow \text{mineralization dye} \quad (6)$$

The degradation of OII ($1.78.10^{-5}$mol/l; pH=6.44) were tested with the prepared samples under UV irradiation with time duration from one hour up to 5 hours. The figure 10 shows the absorbance spectra corresponding to the photo-degradation in the wavelength range from 350 to 600 nm. All spectra present a maximum at an absorption wavelength of 484 nm corresponding to the wavelength of OII. These spectra represented a decrease in absorption with irradiation time. This result indicates that there is a degradation of dye from a clear color up to a transparent color which confirms that these thin films are active catalysts in the photo catalysis application.

The degradation rate after a time t is calculated using the following formula [59]:

$$D(\%) = \frac{A_0 - A_t}{A_0} \times 100 \quad (7)$$

with $A_0$: initial absorption of OII, $A_t$: absorption at time t (t=1 h to 5 h).

All Ag:CuO catalysis system for each doping concentration represented a significant degradation efficiency in the first three hours.The film doped with 50% Ag represented the fastest catalyst. This result shows that the most efficient in the degradation of this dye, corresponding to the degradation rate after 5 h is ~ 43% (Fig.9e). It represents an increase of almost twice compared to a pure CuO with 27% degradation rate for the same time duration.

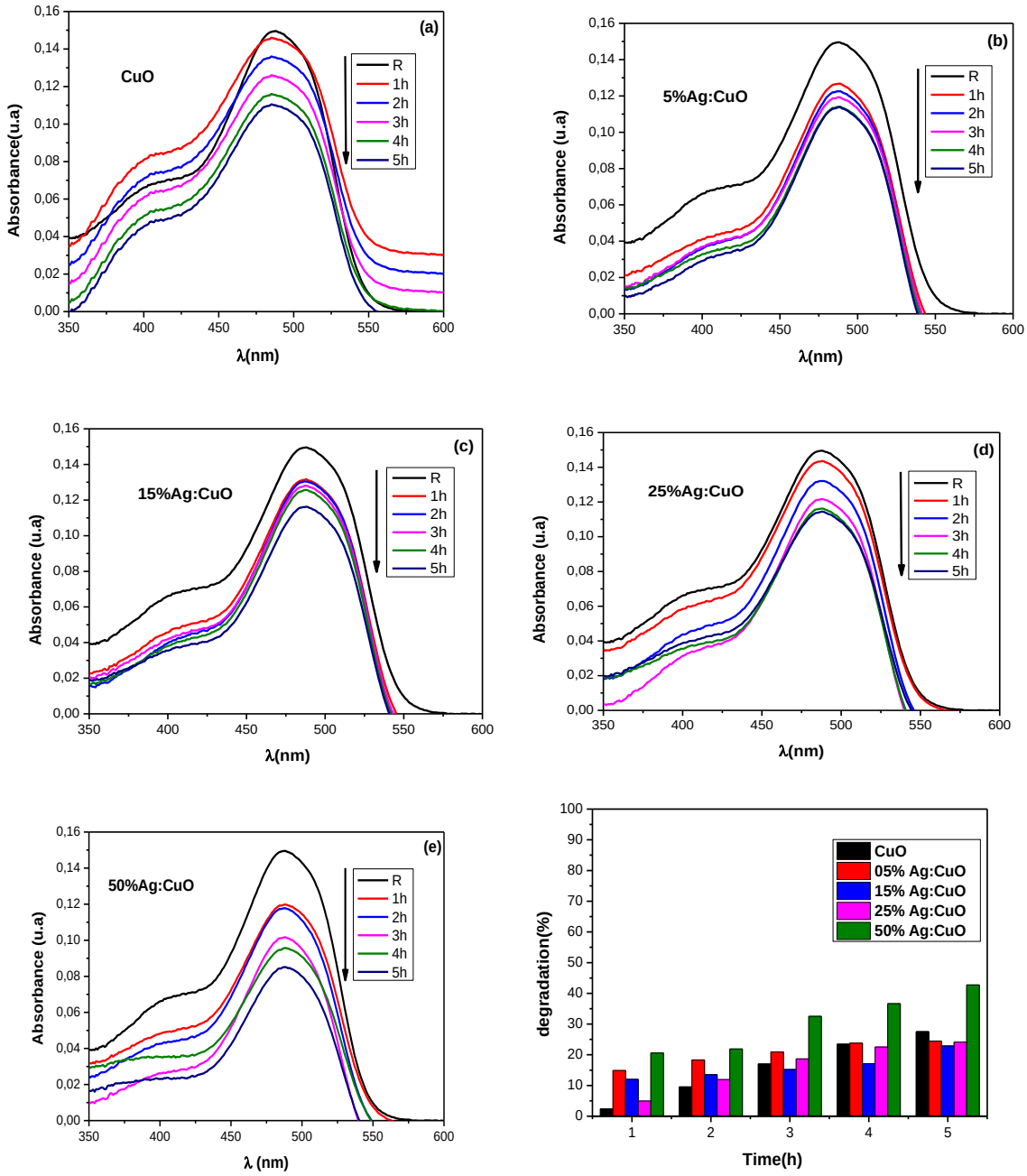


Fig.9. Evolution of UV Visible absorption spectra of OII and their degradation as a fonction of irradiation time with UV light in the presence of thin layers (a): CuO, (b): 5% Ag:CuO, (c): 15 %Ag:CuO, (d): 25%Ag :CuO et (e): 50% Ag:CuO.

Figure 10 shows a significant decrease in the $A/A_0$ ratio for the OII solution as a function of exposure time to UV radiation. The first-order rate constants for OII degradation were estimated using the following equation [58]:

$$A/A_0 = e^{-kt} \quad (8)$$

where: k denotes the rate constant, A and $A_0$ respectively denote initial absorption of OII and absorption at time t (t=1 h to 5 h).

The constant rate for OII dye degradation by pure and 5% doped CuO thin film up to 50% are respectively $6.69.10^{-3}$ $min^{-1}$(pH=6.98), $7.03.10^{-3}$ $min^{-1}$, $6.55 .10^{-3}$ $min^{-1}$, $6.83.10^{-3}$ $min^{-1}$ and $8.23.10^{-3}$ $min^{-1}$(pH=7.11) respectively. These results illustrate the photocatalytic properties of these layers in the decomposition reaction of OII. The faster degradation rate corresponds to the case of 50% Ag doping and reveals that this film with this doping is the most effective catalyst.

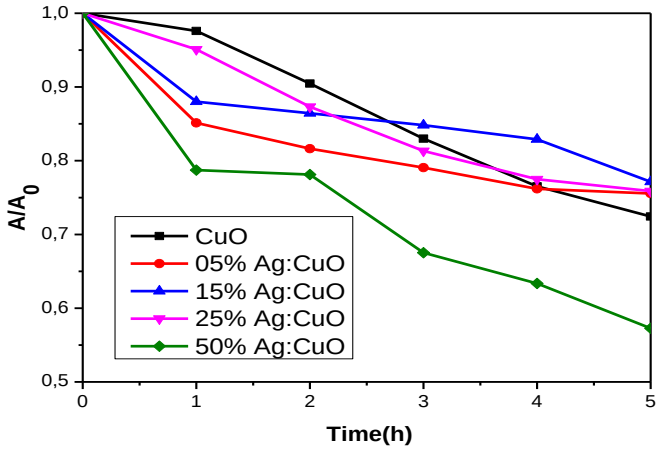


**Fig.10.** ($A/A_0$) as a function of the irradiation time in the presence of thin layers of the Ag: CuO.

### 3.8. Photocatalytic Mechanism

Photocatalysis is an advanced technique that transforms solar energy into sustainable fuels and oxidizes pollutants via the aid of semiconductor photocatalysts. The main scientific and technological challenges for effective photocatalysis are the stability, robustness, and efficiency of semiconductor photocatalysts.

The energy gap of the oxides CuO and $Ag_2O$, estimated at 2.17 eV and 1.31 eV, respectively, enables them to generate electron/hole pairs (e−/h+) While absorbing light energy (Eq.1). Doping CuO with Ag resulted in a decrease in recombination and an increase in optical activity in the visual field. Photo-excitation of Ag:CuO nanoparticles caused electrons to transition from the valence band to the conduction band leaving behind holes, which is called oxidation-reduction reactions. Electrons in the conduction band interact with molecular oxygen to produce superoxide radicalions $\bullet O_2^-$ and hydroperoxyl radicals $\bullet HO_2^-$ (Eq.2), while holes are trapped in the valence band from hydroxyl ions to create OH• radicals (Eq.3) [60]. Creation of more OH• and $\bullet HO_2^-$ resulted in high oxidation factors that contributed to the attack and dissociation of the organic dye molecules (Eq.4 and 5) [46, 60]. The separation and migration mechanism of the photo-generated electron/hole pairs of the Ag:CuO sample isillustrated in the figure 11.

$Ag_2O$ electrons can reduce $O_2$ to $\bullet O_2^-$ due to their positive CB edge potential of -1.16 V with respect to the standard redox potential $E^{\Theta}(O_2/\bullet O_2^-)$ (- 0.33eVvs.NHE) [61]. Thus, the process begins when holes that react with water to produce hydroxide, and electrons react with oxygen to cause a transparent color of the polluted solution. $\bullet O_2^-$ maythen react with $H_2O$ to form $\bullet HO_2$and $H_2O_2$ [62]. Moreover, due to the valence band edgel ocation of CuO oxide (+2.39 eV), there is a possibility of dye oxidation to $CO_2$ and $H_2O$ with CuO through the ementioned holes with respect to thes tandard redox potential $E^{\Theta}(OH^-/\bullet OH)$ (+ 1.99eV vs.NHE) [63]. The position values of two semiconductors at the zero charge point are calculated using the following relations [9, 60]:

$$E_{BV} = X - E_e + 0.5E_g \quad (9)$$

$$E_{BC} = E_{BV} - E_g \quad (10)$$

where $E_{VB}$ is the valence band edge potential, $E_{CB}$ the conduction band edge potential, X the value of electronegativity ($X_{CuO}$ = 5.81 eV [64], $X_{Ag2O}$ = 3.99 eV [65], $E_e$ the energy of free electrons at the hydrogen level (~4.5 eV) and Eg the semiconductor band width. The role of silver doping is very effective compared to the case of CuO. It increases the rate of •OH in a very noticeable way. The formation of holes depends on the chemical nature of Ag:CuO which can explain the high degradation rate of OII in samples with silver doping.The chemical processes are the following:

$$CuO + Ag_2O + h\upsilon \rightarrow CuO\ (e^-) + CuO\ (h^+) + Ag_2O\ (e^-) + Ag_2O\ (h^+) \quad (11)$$

$$Ag_2O\ (e^-) + O_2 + H_2O \rightarrow \bullet O_2^- + \bullet HO_2^- \quad (12)$$

$$CuO\ (h^+) + OH^- + H_2O \rightarrow OH\bullet \quad (13)$$

$$OH\bullet + Dey \rightarrow \text{mineralization dye} \quad (14)$$

$$\bullet O_2^- + \bullet HO_2^- + \text{mineralization dye} \rightarrow CO_2\uparrow + H_2O \quad (15)$$

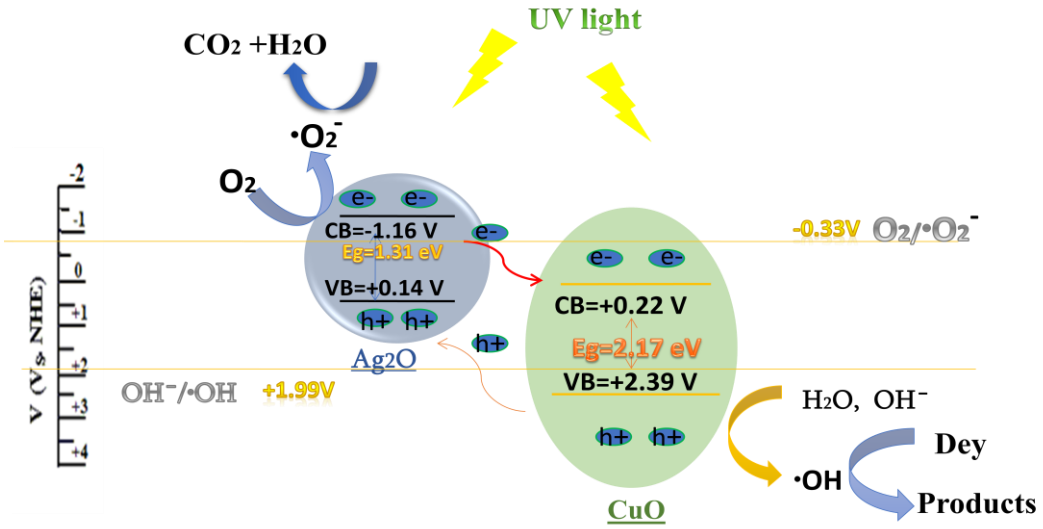


Fig.11.The photocatalytic mechanism of Ag doped CuO thin layers under UV light.

## Conclusion

Thin layers of CuO doped with different percentages of silver (5%, 15%, 25% and 50%) were used to find out their effect as catalysts. A test for the photocatalysis of OII decomposition was done. Thin films were deposited on a glass substrate by sol-gel spin coating method, and the produced films were polycrystalline with a $C_2/c$ space group, with a spectra shift after grafting evidence of a deformation in the copper oxide crystal cell according to XRD data. From SEM results, it was observed that there are pores in the case of Ag doping. Pore number increases with the increase of the doping rate, which gave a very high efficiency and more catalytic surfaces. The creation of pores on the surface of the sample contributed to the deposition of a larger amount of impurities of the polluted solution, which enabled a faster decomposition of the OII dye compared to thin films of pure CuO. This is well confirmed with results of the energy gap which decreases with the increase of the rate of doping due to the increase in energy levels that gives a greater conductivity.

## Acknowledgments

This work has been supported by the Laboratory of Active Components and Materials (LACM) of Larbi Ben M'hidi University - Oum El Bouaghi, Algeria and the laboratory of MOLTECH-Anjou, Angers University, France.

## References

[1] M. Humayunet al.,Recent Progress in the Synthesis and Applications of Composite Photocatalysts: A Critical Review, Small Methods.6(2021) 2101395.

[2] D. Bouras et al., Efficiency of adding DD3+(Li/Mg) composite to plants and their fibers during the process of filtering solutions of toxic organic dyes, Optical Materials.131(2022) 112725.

[3] Q. Wang et al., Particulate photocatalysts for light-driven water splitting: Mechanisms, challenges, and design strategies, Chem. Rev.120(2020) 919–985.

[4] E. R. García et al., Adsorption of Azo-Dye Orange II from Aqueous Solutions Using a Metal-Organic Framework Material: Iron- Benzenetricarboxylate, Materials (Basel).7(2014) 8037–8057.

[5] R. Li et al., Enhancing Hydrogen Adsorption Capacity of Metal Organic Frameworks M(BDC)TED0.5 through Constructing a Bimetallic Structure, ACS Omega.7(2022)20081-20091.

[6] S. Iqbal et al.,Controlled synthesis of Ag-doped CuO nanoparticles as a core with poly(acrylic acid) microgel shell for efcient removal of methylene blue under visible light. Journal of Materials Science: Materials in Electronics.

[7] E. C. Cho et al, Preparation of Ni(OH)2/CuO heterostructures for improved photocatalytic degradation of organic pollutants and microorganism, Chemosphere.300(2022) 134484.

[8] M.V. Landau et al., Conversion of CO2, CO, and H2 in CO2 Hydrogenation to Fungible Liquid Fuels on Fe-Based Catalysts, Industrial &Engineering Chemistry Research . 45(2017)13334-13355.

[9] D. Bouras et al.,Economic and ultrafast photocatalytic degradation of orange II using ceramic powders,Catalysts.11(2021)1-22.

[10] N. Riaz, B. K. Dutta, M. S. Khan, E. Nurlaela, et A. Dhabi, Photocatalytic Degradation of Orange II using Bimetallic Cu-Ni / TiO 2 Photocatalysts, 1(2012) p. 1-5.

[11] L. Ben Ali et al., Dégradation photochimique du colorant alizarine par des nanomatériaux à base de TiO2 ou ZnO tous seuls ou modifiés avec le Pr3+ préparés en milieu polyol (Photochemical degradation of alizarin dye using nanomaterials based on TiO2 or ZnO alone or modified, (2014). https://www.researchgate.net/publication/269574572.

[12] S.S. Shariffudin et al,Preparation and characterization of nanostructured CuO thin films using sol-gel dip coating, IOP Conf. Ser.: Mater. Sci. Eng.99(2015) 012007.

[13] S.K. Hussian,Study of optical properties of copper oxide (CuO) thin film prepared by SPD technique, Muthanna J. Pure Sci. 4(2017)144–152.

[14] B. Dikra et al, Porosity properties of porous ceramic substrates added with zinc and magnesium material, Ceram. Int.46(2020) 20838–20846.

[15] R. D. Prabu et al,An e ff ect of temperature on structural , optical , photoluminescence and electrical properties of copper oxide thin fi lms deposited by nebulizer spray pyrolysis technique , Mater. Sci. Semicond. Process.74(2017) 129-135, 2018.

[16] S.S. Shariffudin et al,Preparation and characterization of nanostructured CuO thin films using sol-gel dip coating, IOP Conf. Ser.: Mater. Sci. Eng.99(2015)012007.

[17] R.R. Prabhu, A.C. Saritha, M.R. Shijeesh, M.K. Jayaraj, Fabrication of p-CuO/n-ZnO heterojunction diode via sol-gel spin coating Technique, Mater. Sci. Eng.220(2017) 82–90.

[18] Zi-Y. Chen et al,Suppressing the Agglomeration of ZnO Nanoparticles in Air by Doping with Lower Electronegativity Metallic Ions: Implications for Ag/ZnO Electrical Contact Composites, ACS Applied Nano Materials.5(2022)10809-10817.

[19] A. N. Ahmed et al,Effect of Process Variables on Deposited Cupric Oxide Thin Film by Sol-Gel Spin Coating Technique Effect of Process Variables on Deposited Cupric Oxide Thin Film by Sol- Gel Spin Coating Technique ,(2018).

[20] N. Thakur et al,Effect of (Ag, Co) co-doping on the structural and antibacterial efficiency of CuO nanoparticles: A rapid microwave assisted method», Journal of Environmental Chemical Engineering. 8(2020)104011.

[21] Z. Xieet al,Effect of impurity in Cu2O nanowires on the degradation of methyl orange, J. Mater. Sci.: Mater. Electron.31(2020) 3817–3824.

[22] L. Zhang et al,N-doped nanoporous graphene decorated three-dimensional CuO nanowire network and its application to photocatalytic degradation of dyes , RSC Adv. 4(2014) 47455-47460.

[23] M. Borgwardt et al., « Femtosecond time-resolved two-photon photoemission studies of ultrafast carrier relaxation in Cu2O photoelectrodes»,Nature Communications, 10(2019).

[24] H. Hashim, S. S. Shariffudin, P. S. M. Saad, et H. A. M. Ridah, Electrical and Optical Properties of Copper Oxide Thin Films by Sol-Gel Technique , IOP Conf. Ser. Mater. Sci. Eng.99(2015).

[25] D. Rania, A. Rabah, T. Mamadou, et M. Christine, Elaboration de nanomatériaux fonctionnels pour des applications biomédicales , (2017)1-11.

[26] U. G. Akpan et B. H. Hameed, The advancements in sol – gel method of doped-TiO 2 photocatalysts,375(2010) 1-11.

[27] K. K. H. S. Z. Sadeghi, A comparative investigation on growth , nanostructure and electrical properties of copper oxide thin films as a function of annealing conditions , 2014.

[28] M. Maraj, A. Raza, X. Wang, J. Chen, K. N. Riaz, et W. Sun, Mo-doped CuO Nanomaterial for Photocatalytic Degradation of Water Pollutants Under Visible Light,(2021) 1-11.

[29] L. Sun et al,Nitrogen-Doped Carbon-Coated CuO-In2O3 p–n Heterojunction for Remarkable Photocatalytic Hydrogen Evolution , Adv. Energy Mater., 9(2019) 1-11.

[30] M. R. Johan, M. Shahadan, M. Suan, N. L. Hawari, et H. A. Ching, Annealing Effects on the Properties of Copper Oxide Thin Films Prepared by Chemical Deposition,6(2011) 6094-6104.

[31] S. Kose, F. Atay, V. Bilgin, et I. Akyuz, Some physical properties of copper oxide films : The effect of substrate temperature, 111(2008)351-358.

[32] J. F. P. and S. U. Department P Narayana Reddy, M Hari Prasad Reddy, Characterization of silver oxide films formed by reactive RF sputtering at different substrate .

[33] A. M. El Sayed et M. Shaban, Structural, optical and photocatalytic properties of Fe and (Co, Fe) co-doped copper oxide spin coated films, Spectrochim. ACTA PART A Mol. Biomol. Spectrosc,149(2015) 638-646.

[34] M. Science-poland, Fabrication and characterization of Zn doped CuO nanofiber using newly designed nanofiber generator for the photodegradation of methylene blue from textile effluent,36(2018) 520-529.

[35] M. R. H. SIDDIQUI et R. A. and A. A.-W, S.F. ADIL, M.E. ASSAL,Synthesis and Characterization of Silver Oxide and Silver Chloride Nanoparticles with High Thermal Stability, 25(2013) 3405-3409.

[36] S. M. Hosseini, I. A. Sarsari, P. Kameli, et H. Salamati, Effect of Ag doping on structural, optical, and photocatalytic properties of ZnO nanoparticles , J. Alloys Compd., 640(2015) 408-415

[37] H. A. Thabit et al.,Development of Ag-Doped ZnO Thin Films and Thermoluminescence (TLD) Characteristics for Radiation Technology», Nanomaterials (Basel)., 12 (2022)3068.

[38] Zhou F et al, Doping Ag in ZnO Nanorods to Improve the Performance of Related Enzymatic Glucose Sensors, Sensors.17(2017) 2214.

[39] Zi-Y. Chen et al., Tuning the interface adhesion of Ag/ZnO composites by metallic dopants: A DFT study, Computational Materials Science.224 (2023) 112151.

[40] X. Wang et al,Ag2O as a New Visible-Light Photocatalyst: Self-Stability and High Photocatalytic Activity, Chemistry - A European Journal. 17(2011)7777-80.

[41] T. L. Xinqiang Zhang et al,Targeting inside charge carriers transfer of photocatalyst: Selective deposition of Ag2O on BiVO4 with enhanced UV–vis-NIR photocatalytic oxidation activity, Applied Catalysis B: Environmental,251(2019) 220-228.

[42] M. Nesa, M. Sharmin, K. S. Hossain, et A. H. Bhuiyan, Structural, morphological, optical and electrical properties of spray deposited zinc doped copper oxide thin films , J. Mater. Sci. Mater. Electron. 28 (2017)12523-12534.

[43] E. Benrezgua et al, Synthesis and properties of copper doped zinc oxide thin films by sol-gel , spin coating and dipping : A characterization review , J. Mol. Struct. 1267(2022)133639.

[44] S. Das et T. Alford, Structural and optical properties of Ag-doped copper oxide thin films on polyethylene napthalate substrate prepared by low temperature microwave annealing, (2013).

[45] N. D. Dinesh et K. Kumar, Synthesis of CuO and Ag doped CuO nanoparticles from Muntingia calabura leaf extract and evaluation of their antimicrobial potential,(2019).

[46] D. Bouras et al,Cu:ZnO deposited on porous ceramic substrates by a simple thermal method for photocatalytic application, Ceram. int.44(2018)21546–21555.

[47] H. Hussin, R. Salam, R. Jasim, et N. F. Habubi, Optical and Structural Properties of Nanostructured CuO Thin Films Doped by Mn .(2020).

[48] R. Sharma, S.L. Patel, M. D. Kannan, et M. S. Dhaka, Effect of different annealing conditions on CdZnTe thin films for absorber layer applications , Surfaces and Interfaces. 33(2022)102204.

[49] R. Marnadu et al,Significant enhancement in photosensitivity, responsivity, detectivity and quantum efficiency of Co3O4 nanostructured thin film-based photodetectors through Mo doping developed by spray pyrolysis method , Surfaces and Interfaces.34(2022)102366. https://doi.org/ 10.1016/j.surfin.2022.102366

[50] A. B. Bodade, M. A. Taiwade, et G. N. Chaudhari, Bioelectrode based chitosan-nano copper oxide for application to lipase biosensor , J. Appl. Pharm. Res. 5(2017)30-39,

[51] M. F. A. Aboud, S. Haider, et M. F. Warsi, Fabrication of Binary Metal Doped CuO Nanocatalyst and Their Application for the Industrial Effluents Treatmen , Ceram. Int.(2020).https://doi.org/10.1016/j.ceramint.2020.11.064

[52] L. Radev, I. Michailova, D. Zaimova, et T. Dimova, In vitro bioactivity of Silver containing sol-gel glasses : FTIR analysis,Imp.J.Interdiscip.Res(2017) 316-323.

[53] M. G. Méndez-Medrano et al.Surface Modification of TiO2 with Ag Nanoparticles and CuO Nanoclusters for Application in Photocatalysis, J. Phys. Chem.120 (2016)5143-5154.https://doi.org/10.1021/acs.jpcc.5b10703

[54] N. Mukherjee et al.CuO nano-whiskers: Electrodeposition, Raman analysis, photoluminescence study and photocatalytic activity, Mater. Lett. 65 (2011) 3248-3250. doi:10.1016/j.matlet.2011.07.016

[55] X. Chenet al, Cu2O nanoparticles and multi-branched nanowires asanodes for lithium-ion batteries, NANO 13.(2018)1850103.

[56] M. F. A. Aboud, S. Haider, et M. F. Warsi, Fabrication of Binary Metal Doped CuO Nanocatalyst and Their Application for the Industrial Effluents Treatmen , Ceram. Int.(2020).

[57] K. Sahu, S. Choudhary, S. A. Khan, et A. Pandey,Thermal evolution of morphological , structural , optical and photocatalytic properties of CuO thin films ,Nano-Structures & Nano-Objects.17(2019)92-102.

[58] S. Lacombe et al, La photocatalyse pour l'élimination des polluants, Actual .Chim.(2007)79-93.

[59] B. Dikra et al, High photocatalytic capacity of porous ceramic-based powder doped with MgO, Journal of the Korean Ceramic Society. 60( 1) (2023) 155-168. https://doi.org/ 10.1007/s43207-022-00254-5.

[60] D. Bouras et al, Comparison between CrZO and AlZO thin layers and the effect of doping on the lattice properties of zinc oxide, Optical and Quantum Electronics (2022) 54-824. https://doi.org/10.1007/s11082-022-04161-1

[61] M.M. Najafpour, A.N. Moghaddam, H. Dau, I. Zaharieva, Fragments of Layered Manganese Oxide Are the Real Water Oxidation Catalyst after Transformation of Molecular Precursor on Clay J. Am. Chem. Soc. 136 (2014)7245-7248.

[62] I. Khan, M. Luo, S. Khan, H. Asghar, M. Saeed, S. Khan, A. Khan, M. Humayun, L. Guo, B. Shi, Green synthesis of SrO bridged LaFeO3/g-C3N4 nanocomposites for CO2 conversion and bisphenol A degradation with new insights into mechanism. Environ.Res.7, 112650 (2022). doi: 10.1016/j.envres.2021.112650.

[63] M. Wiechen, M.M. Najafpour, S.I. Allakhverdiev, L. Spiccia, Water oxidation catalysis by manganese oxides: learning from evolution Energy Environ. Sci. 7(2014)2203-2212.

[64] J. He et al, Performance promotion of $Ag_2O$ photocatalyst by particle size and crystal surface regulation, New Journal of Chemistry.25(2020).

[65] H. Xu et al,The formation of visible light-driven Ag/Ag2O photocatalyst with excellent property of photocatalytic activity and photocorrosion inhibition, Journal of Colloid and Interface Science.516 (2018)511-521.